Ion-Exchange Behavior of One-Dimensional Linked Dodecaniobate Keggin Ion Materials

May Nyman,*,† Craig R. Powers,‡ Francois Bonhomme,† Todd M. Alam,† Edward J. Maginn,‡ and David T. Hobbs§

Sandia National Laboratories, Albuquerque, New Mexico 87185, Department of Chemistry & Biomolecular Engineering, University of Notre Dame, Notre Dame, Indiana 46556, and Savannah River National Lab, Washington Savannah River Company, Aiken, South Carolina 29808

Received November 27, 2007. Accepted January 22, 2008

Ion-exchange media for cation or anion separations are employed in private industries such as mining, pharmaceutical, and chemical. Government organizations utilize ion-exchange processes for water treatment, environmental remediation and preservation, and nuclear waste treatment. Here, we present an investigation of the ion-exchange behavior of polyoxoniobate materials. Dodecaniobate Keggin ions, $[TNb_{12}O_{40}]^{16-}$ (T = Si, Ge) linked by cationic dimer bridges, $[Nb_2O_2]^{6+}$ or $[Ti_2O_2]^{4+}$ form a one-dimensional anionic framework, charge-balanced by hydrated Na^+ cations. The hydrated sodium resides in interchain tunnels, only loosely associated with the Keggin chains, a geometry that provides rapid exchange kinetics and high exchange capacity. The lattice water is extremely mobile and could not be located on fixed crystallographic positions. Rather, we characterized the water loading by both thermogravimetric studies and computational studies. The LeBail method was used to quantify unit cell change of Keggin chain materials in which the sodium was exchanged completely with Sr^{2+}, Cd^{2+}, and Yb^{3+}. We located Sr^{2+} sites in the Sr-exchanged phase by Rietveld refinement. Ideal sites for Sr^{2+} in the interchain space were also predicted by computational studies, and the experimental and theoretical results were compared. Finally, we investigated the selectivity of the Keggin-chain phases for sorption of radionuclides Sr, Np, and Pu from high ionic strength, highly caustic simulants for Savannah River Site's nuclear wastes.

Introduction

Polyoxometalates (POMs) are discrete, anionic metal-oxo clusters of the early d-0 transition metal octahedra (predominantly VO_6, NbO_6, MoO_6, and WO_6). These nanometer-sized building blocks, under appropriate conditions, can self-assemble into ordered materials with unique structures and oftentimes exploitable functions.[1,2] Applications include heterogeneous catalysis, ion exchange, separation and storage of small molecules, magnetism, and photochromic or electrochromic response. The geometry and chemistry of POM clusters are in some aspects ideal for controlled materials assembly. In particular, both the plenary (complete) and lacunary (incomplete) POMs can serve as multidentate ligands to a variety of metal cations including transition metals,[3–7] lanthanides,[8–10] and alkalis.[11,12] The metal cations, in turn, bridge multiple clusters, completing complex assemblies of alternating cluster anions and metal cations. The structure of the resulting material depends on the arrangement of multiple binding sites in the cluster, the geometry of the binding site(s), preferred bonding geometry of the linking metal cation, and addition of other ligands to complete the coordination sphere of the metal cation linkers. A huge variety of POM-based materials have been recognized that are composed of these ionic building blocks, including one-dimensional straight chains,[3,6,9,12] zigzag chains,[4,8,9,11] two-dimensional linkages,[6] and three-dimensional materials.[5,13,14]

In the relatively more recent development of polyoxoniobate (PONb) chemistry, it has been noted that the niobate clusters have a greater tendency toward the formation of linked POM materials than isolated and soluble salts. Some examples include straight chains of Keggin ions $[XNb_{12}$-

* Corresponding author. E-mail: mdnyman@sandia.gov.
† Sandia National Laboratories.
‡ University of Notre Dame.
§ Washington Savannah River Company.

(1) Long, D. L.; Burkholder, E.; Cronin, L. *Chem. Soc. Rev.* **2007**, *36*, 105–121.
(2) Katsoulis, D. E. *Chem. Rev.* **1998**, *98*, 359–387.
(3) Wang, J. P.; Du, X. D.; Niu, J. Y. *Chem. Lett.* **2006**, *35*, 1408–1409.
(4) Nogueira, H. I. S.; Paz, F. A. A.; Teixeira, P. A. F.; Klinowski, J. *Chem. Commun.* **2006**, 2953–2955.
(5) Gao, B.; Liu, S. X.; Xie, L. H.; Yu, M.; Zhang, C. D.; Sun, C. Y.; Cheng, H. Y. *J. Solid State Chem.* **2006**, *179*, 1681–1689.
(6) Lisnard, L.; Dolbecq, A.; Mialane, P.; Marrot, J.; Codjovi, E.; Secheresse, F. *Dalton Trans.* **2005**, 3913–3920.
(7) Khan, M. *J. Solid State Chem.* **2000**, *152*, 105–112.
(8) Sadakane, M.; Dickman, M. H.; Pope, M. T. *Angew. Chem., Int. Ed.* **2000**, *39*, 2914–2916.
(9) Wang, J. P.; Duan, X. Y.; Du, X. D.; Niu, J. Y. *Cryst. Growth Des.* **2006**, *6*, 2266–2270.
(10) Mialane, P.; Dolbecq, A.; Secheresse, F. *Chem. Commun.* **2006**, 3477–3485.
(11) Fan, L. H.; Xu, L.; Gao, G. G.; Li, F. Y.; Li, Z. K.; Qiu, Y. F. *Inorg. Chem. Commun.* **2006**, *9*, 1308–1311.
(12) Chang, S.; Qin, C.; Wang, E. B.; Li, Y. G.; Wang, X. L. *Inorg. Chem. Commun.* **2006**, *9*, 727–731.
(13) Zhang, X. T.; Wang, D. Q.; Dou, J. M.; Yan, S. S.; Yao, X. X.; Jiang, J. Z. *Inorg. Chem.* **2006**, *45*, 10629–10635.
(14) Wang, X. L.; Qin, C.; Wang, E. B.; Su, Z. M.; Li, Y. G.; Xu, L. *Angew. Chem., Int. Ed.* **2006**, *45*, 7411–7414.

10.1021/cm800158u CCC: $40.75
Published on Web 03/11/2008

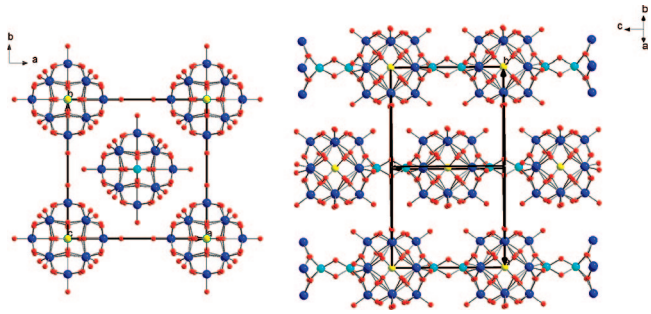

Figure 1. Two views of the Keggin-chain ion-exchange materials. Red is oxygen, dark blue is niobium, light blue is Ti or Nb of the bridging units, yellow is Si or Ge, central to the Keggin clusters. Extra-framework cations and water molecules are not shown. On the left is the view down the chain-axis (*c*-axis) and on the right is the parallel chains observed down the (110) axis.

$O_{40}]^{16-}$ (X = Si, Ge) linked by $[Ti_2O_2]^{4+}$ or $[Nb_2O_2]^{6+}$,[15,16] layers of $[GeNb_{12}O_{40}]^{16-}$ linked in orthogonal directions by K^+ and $[Nb_2O_2]^{6+}$,[17] $[P_4Nb_9O_{40}]^{15-}$ linked into layers by Na^+,[18] and $[Nb_6O_{19}]^{8-}$ CuL_x zigzag and straight-chain complexes (L = amines).[19] All of the linked polyoxoniobate Keggin ion phases have alkali counterions and lattice water that is interstitial to the low-dimensional "framework", and the Keggin-chain phases $Na_{12}[Ti_2O_2][TNb_{12}O_{40}]\cdot xH_2O$ and $Na_{10}[Nb_2O_2][TNb_{12}O_{40}]\cdot xH_2O$ (T = Si, Ge) have very mobile extra-framework species and a flexible framework that is connected only in one direction.[15] Consequently, these compounds are readily ion-exchanged, both rapidly and with high exchange capacity. Figure 1 provides two views of the Keggin chains with the cations and extra-framework water molecules removed for ease of viewing. This figure illustrates the one-dimensional linkage of the clusters and interchain region where the mobile cations and water molecules reside.

We have investigated general ion-exchange behavior of the Keggin chain materials; in particular, separation and sequestration of radionuclides from nuclear wastes such as the highly caustic, high ionic strength wastes stored at the Savannah River Site.[20] These materials are potentially useful for this application for two reasons. First, related polyoxotungstate clusters coordinated to actinyl ions have been characterized, illustrating the coordination ability of POMs to actinides.[21–23] However, unlike most of the related polyoxotungstate, polyoxomolybdate, and polyoxovanadate phases, the polyniobates are base-stable, and therefore should be less likely to decompose in the highly alkaline conditions of the nuclear wastes. In this study, we characterize ion-exchange products of the Keggin-chain materials using both experimental and computational methods. We also report their selectivity and sorption kinetics of three radionuclides, strontium, neptunium, and plutonium, from Savannah River Site (SRS) nuclear waste simulants.

Experimental Section

Preparation and Characterization of Ion-Exchanged Phases. The sodium form of the Keggin-chain phases were synthesized as previously reported.[15] Using the same nomenclature from prior publication, these phases are referred to as: $Na_{12}[Ti_2O_2][SiNb_{12}O_{40}]\cdot xH_2O$ (**Ti-Si-Nb**), $Na_{12}[Ti_2O_2][GeNb_{12}O_{40}]\cdot xH_2O$ (**Ti-Ge-Nb**), $Na_{10}[Nb_2O_2][SiNb_{12}O_{40}]\cdot xH_2O$ (**Nb-Si-Nb**), and $Na_{10}[Nb_2O_2][GeSiNb_{12}O_{40}]\cdot xH_2O$ (**Nb-Ge-Nb**), where the first element is in the $[M_2O_2]$ (M = Ti, Nb) bridging site linking the Keggin ions, the second element (Si or Ge) is in the central tetrahedral site of the Keggin ion, and the third (Nb) is the metal of the Keggin ion. Ion exchange of Sr^{2+}, Cd^{2+}, and Yb^{3+}were carried out as follows: 0.1 molar solutions of the nitrate salts were prepared by dissolving the appropriate amount of salt in 40 mL of deionized water: $Sr(NO_3)_2$ (0.85 g) $Cd(NO_3)_2\cdot 4H_2O$ (1.23 g), $Yb(NO_3)_3\cdot 5H_2O$ (1.80 g) along with 30 mg of the native sodium form of the Keggin-chain material for ion exchange, and shaking on a shaker table at room temperature for two hours. The ion-exchanged solids were then isolated by centrifuging, rinsing, and drying in a vacuum oven. Ion-exchanged samples were characterized by SEM-EDS (Scanning electron microscopy-energy dispersive spectroscopy) for qualitative determination of completeness of ion exchange, ICP-MS (inductively coupled plasma-mass spectroscopy) for quantitative determination of exchange, and thermogravimetric analysis (TGA) to determine water content of exchanged samples.

X-ray Data Collection and Structure Refinement. X-ray powder diffraction data were collected on ion exchanged phases, after complete exchange was confirmed by elemental analysis techniques. X-ray powder diffraction data were collected on a Siemens D500 equipped with a Kevex detector. Samples for X-ray diffraction were first mixed with an internal standard (Si SRM640, $a = 5.430898$ Å) by grinding with a mortar and pestle and smear-mounted on a flat glass plate. X-ray data was collected from 5 to 90°, 0.04° step size, and 12 or 25 s step time. Upon exchange of sodium for Sr, Yb, or Cd, the Keggin chain phase did not undergo any alteration in symmetry, just a change in the unit-cell volume. Therefore, the structures of the exchanged phases were refined in the same space group as the native Na-forms, tetragonal *I*–4*m*2 (No. 119). The structure of Sr exchanged **Ti-Si-Nb** was refined using the Rietveld method.[24] The distance and angle restraints that were applied to structure solution of the native Na form of **Ti-Si-Nb** were also applied to the ion-exchanged phases.[15] Four extra-framework sites were found and optimized as (1) fully occupied with strontium, (2) ½ occupied with strontium, (3) ¼ occupied with strontium, and (4) fully occupied with water. For the Sr-exchanged **Ti-Ge-Nb**, **Nb-Si-Nb**, and **Nb-Ge-Nb**, unit-cell parameters were determined by the LeBail method.[24] Full refinements were not performed; the relative chemical instability of these phases resulted in poorer-quality X-ray data. Rietveld refinement was also performed on Cd-exchanged **Ti-Si-Nb** and Yb-exchanged **Ti-Si-Nb**. Unit-cell parameters and R_{Bragg} for all ion exchange phases are

(15) Bonhomme, F.; Larentzos, J. P.; Alam, T. M.; Maginn, E. J.; Nyman, M. *Inorg. Chem.* **2005**, *44*, 1774–1785.
(16) Nyman, M.; Bonhomme, F.; Alam, T. M.; Rodriguez, M. A.; Cherry, B. R.; Krumhansl, J. L.; Nenoff, T. M.; Sattler, A. M. *Science* **2002**, *297*, 996–998.
(17) Nyman, M.; Larentzos, J. P.; Maginn, E. J.; Welk, M. E.; Ingersoll, D.; Park, H.; Parise, J. B.; Bull, I.; Bonhomme, F. *Inorg. Chem.* **2007**, *46*, 2067–2079.
(18) Nyman, M.; Celestian, A. J.; Parise, J. B.; Holland, G. P.; Alam, T. M. *Inorg. Chem.* **2006**, *45*, 1043–1052.
(19) Bontchev, R. P.; Venturini, E. L.; Nyman, M. *Inorg. Chem.* **2007**, *46*, 4483–4491.
(20) Hunt, R. D.; Collins, J. L.; Adu-Wusu, K.; Crowder, M. L.; Hobbs, D. T.; Nash, C. A. *Sep. Sci. Technol.* **2005**, *40*, 2933–2946.
(21) Antonio, M. R.; Williams, C. W.; Soderholm, L. *J. Alloys Compd.* **1998**, *271*, 846–849.
(22) Chiang, M. H.; Williams, C. W.; Soderholm, L.; Antonio, M. R. *Eur. J. Inorg. Chem.* **2003**, *14*, 2663–2669.
(23) Williams, C. W.; Antonio, M. R.; Soderholm, L. *J. Alloys Compd.* **2000**, *303*, 509–513.
(24) Rodriguez-Carvajal, J. FULLPROF: A Program for Rietveld Refinement and Pattern Matching Analysis. *Abstracts from the Satellite Meeting on Powder Diffraction of the XVth Congress of the IUCr.*, Toulouse, France; International Union of Crystallography: Geneva, Switzerland, 1990.

Table 1. Unit-Cell Parameters[a] of Keggin-Chain Materials in Their Ion-Exchanged and Native forms

phase	*a* (Å) (error)	(*c*) Å (error)	*V* (Å^3) (error)	R_{Bragg} (%)
Ti-Si-Nb_native[b]	14.2701(5)	11.2923(7)	2299.5(2)	N/A
Ti-Si-Nb_Sr	14.623(1)	11.545(1)	2469(1)	1.51
Ti-Si-Nb_Cd	13.940(1)	11.192(1)	2175(1)	4.93
Ti-Si-Nb_Yb	14.231(1)	11.392(1)	2307(1)	3.25
Ti-Ge-Nb_native[b]	14.2852(5)	11.3222(7)	2310.5(2)	N/A
Ti-Ge-Nb_Sr	14.655(5)	11.561(3)	2483(2)	1.73
Nb-Si-Nb_native[b]	14.2649(5)	11.3575(7)	2311.1(1)	N/A
Nb-Si-Nb_Sr	14.612(1)	11.682(1)	2494(1)	1.76
Nb-Ge-Nb_native[b]	14.2633(5)	11.3947(7)	2318.2(1)	N/A
Nb-Ge-Nb_Sr	14.638(2)	11.692(2)	2505(2)	1.73

[a] All refined in the tetragonal space group, $I-4m2$ (No. 119). [b] From ref 15.

Table 2. Atomic positions for Ti-Si-Nb-native[b] and Ti-Si-Nb_Sr[a]

atom	phase	*x*	*y*	*z*	population (%)
Nb1	Ti-Si-Nb-native	0.8704(3)	0.1335(3)	0.2163(2)	
	Ti-Si-Nb_Sr	0.8761(5)	0.1241(4)	0.2130(5)	
Nb2	Ti-Si-Nb-native	0	0.2568(2)	0.9976(6)	
	Ti-Si-Nb_Sr	0	0.2510(4)	0.9963(9)	
Ti	Ti-Si-Nb-native	0	0	0.3701(4)	
	Ti-Si-Nb_Sr	0	0	0.3731(8)	
Si	Ti-Si-Nb-native	0	0	0	
	Ti-Si-Nb_Sr	0	0	0	
O1	Ti-Si-Nb-native	0	0.3836(6)	0.005(6)	
	Ti-Si-Nb_Sr	0	0.354(3)	0.077(7)	
O2	Ti-Si-Nb-native	0.837(1)	0.202(1)	0.339(1)	
	Ti-Si-Nb_Sr	0.855(5)	0.186(4)	0.343(2)	
O3	Ti-Si-Nb-native	0	0.118(1)	0.274(2)	
	Ti-Si-Nb_Sr	0	0.121(1)	0.288(2)	
O4	Ti-Si-Nb-native	0	0.886(1)	0.735(2)	
	Ti-Si-Nb_Sr	0	0.879(1)	0.712(2)	
O5	Ti-Si-Nb-native	0.7572(9)	0.090(1)	0.135(1)	
	Ti-Si-Nb_Sr	0.761(1)	0.087(4)	0.136(4)	
O6	Ti-Si-Nb-native	0.236(1)	0.892(1)	0.896(2)	
	Ti-Si-Nb_Sr	0.164(3)	0.906(2)	0.946(1)	
O7	Ti-Si-Nb-native	0.0970(5)	0	0.0833(9)	
	Ti-Si-Nb_Sr	0.0954(5)	0	0.0754(9)	
O8	Ti-Si-Nb-native	0.081(1)	0	0.5	50
	Ti-Si-Nb_Sr	0.081(1)	0	0.5	
site 1[c]	Ti-Si-Nb-native	0.747(1)	0.253(-)	0	100
Sr1	Ti-Si-Nb_Sr	0.2391(8)	0.2391(-)	0.5	100
site 2[c]	Ti-Si-Nb-native	0.394(1)	0.106(-)	0.25	100
Sr2	Ti-Si-Nb_Sr	0	0.5	0.134(4)	50
site 3[c]	Ti-Si-Nb-native	0.267(2)	0.041(2)	0.458(3)	50
Sr3	Ti-Si-Nb_Sr	0	0.234(4)	0.589(7)	25
site 4[c]	Ti-Si-Nb-native	0.099(2)	0.458(2)	0.164(3)	50
O_{water}	Ti-Si-Nb_Sr	0.245(1)	0.255(1)	0.25	100

[a] Isotropic atomic displacement parameters for Ti-Si-Nb-native: B(Nb) = B(Ti) = B(Si) = 2.9(1) Å^2; B(O) = 3.0(3) Å^2; B(Na/H_2O) = 6.0(4) Å^2. Isotropic atomic displacement parameters for Ti-Si-Nb-Sr-exchange: B(Nb) = B(Ti) = B(Si) = B(O) = 2.5(1) Å^2; B(Sr) = B(H_2O) = 7.5(5) Å^2. [b] From ref 15. [c] Extraframework Na/H_2O sites (see ref 15).

summarized in Table 1. Table 2 gives the atomic positions of the native Na form of Ti-Si-Nb and the Sr-exchanged Ti-Si-Nb, for comparison. The atomic positions of the other exchanged phases can be found in the CIF files in the Supporting Information.

^{113}Cd NMR. The ^{113}Cd MAS NMR spectra were obtained on a Bruker AMX400 instrument at 88.80 MHz using a 4 mm broadband MAS probe spinning at 12 kHz. Spectra were obtained using a single pulse Bloch decay with a 10 s recycle delay and 512 scans. The ^{113}Cd chemical shifts was referenced to the secondary external standard 1 M $Cd(ClO_4)_2$ δ 0.0.

Computational Methods. A (2X2X2) supercell was constructed from the experimental crystal structure. Partially populated sites were filled randomly, with minimum spacing rules to attempt to minimize cation–cation and oxygen−oxygen interaction energy. The fractional population was applied over the entire supercell.

Table 3. Interaction Parameters for Simulation of 100% Sr-Exchanged Ti-Si-Nb

interaction	σ (Å)	ϵ/k_B (K)
$Sr-O_{framework}$	3.139	68.210
$Sr-O_{water}$	3.139	68.210
$O_{water}-O_{framework}$	3.169	78.201
$O_{water}-O_{water}$	3.169	78.201

Table 4. Partial Charges for Simulation of 100% Sr-Exchanged Ti-Si-Nb

species	charge (*e*)
Nb	+3.39
Ti	+2.14
Si	+3.30
O_{fw} (2 Nb)	−1.49
O_{fw} (3 Nb)	−1.53
O_{fw} (bridge)	−1.45
O_{fw} (Si)	−1.54
O_{fw} (terminal)	−1.26
Sr	+2.00

The force field for the simulations is a pairwise potential combining a Lennard−Jones dispersion/repulsion term and a Coulombic point charge interaction term,

$$u_{ij} = 4\epsilon_{ij}\left(\left(\frac{\sigma_{ij}}{r_{ij}}\right)^{12} - \left(\frac{\sigma_{ij}}{r_{ij}}\right)^{6}\right) + \frac{q_i q_j}{r_{ij}}$$

where u_{ij} is the potential for a pair of sites i and j separated by a distance r_{ij}, σ_{ij} and ϵ_{ij} are Lennard−Jones parameters, and q_i and q_j are the point charges for sites i and j, respectively. The same form was used for interactions involving the framework, adsorbates, and cations. The crystal was modeled with Lennard−Jones sites at only the exposed oxygen atoms, but with Coulombic sites at all atoms. Water was modeled using the rigid simple point charge (SPC) model.[25,26] The parameters for Sr^{2+}−SPC interactions[27] were fitted to free energies of hydration. The framework oxygen Lennard−Jones parameters were taken as identical to the SPC oxygen for water−framework and cation−framework interactions. The point charges for the framework were obtained using plane-wave density functional theory calculations.[28] A complete listing of force field parameters and partial charges is given in Tables 3 and 4. The simulation was carried out using three-dimensional periodic boundary conditions. A cutoff of 11.5 Å was used for the Lennard−Jones terms. Long-range electrostatic interactions were computed using the Ewald summation method,[29] with a 11.5 Å real-space cutoff, an h-vector cutoff of 3.75 Å^{-1}, and a damping factor of 0.3478.

Monte Carlo simulations sampling the grand canonical ensemble[30] were performed to obtain the water adsorption isotherm at 300 K. A total of 75 million steps were carried out, with the first 55 million discarded for equilibration. A full set of data points was obtained with the cations fixed at their crystallographic positions. A single simulation was also performed at saturation where cation motion was sampled using conventional Monte Carlo translation moves. Although simple Monte Carlo does not provide

(25) Jorgensen, W. L.; Chandrasekhar, J.; Madura, J. D.; Impey, R. W.; Klein, M. L. *J. Chem. Phys.* **1983**, *79*, 926–935.
(26) Berendsen, H. J. C.; Postma, J. P. M.; Gunsteren, W. F. v.; Hermans, J. In *Intermolecular Forces*; Pullman, B., Ed.; Reidel: Dordrecht, Netherlands, 1981.
(27) Åqvist, J. *J. Phys. Chem.* **1990**, *94*, 8021–8024.
(28) Larentzos, J. P. Private communication.
(29) Wheeler, D. R.; Fuller, N. G.; Rowley, R. L. *Mol. Phys.* **1997**, *92*, 55–62.
(30) Frenkel, D.; Smit, B. *Understanding Molecular Simulation: From Algorithms to Applications*; Academic Press: New York, 2002.

Table 5. Monte Carlo Move Probabilities

mobile cations		fixedcations	
move type	probability (%)	move type	probability (%)
translate	45	translate	30
rotate	45	rotate	60
insert	5	insert	5
delete	5	delete	5

Table 6. Chemical and Radiochemical Composition of Savannah River Site Simulated Waste Solution

component	concentration
NaOH	1.33 M
total $NaNO_3$	2.6 M
$NaAl(OH)_4$	0.429 M
$NaNO_2$	0.134 M
Na_2SO_4	0.521 M
Na_2CO_3	0.026 M
total Na	5.6 M
stable strontium	298 ± 9.53 μg/L
Sr-85	$9.80 \pm 0.31 \times 10^{-4}$ dpm/mL
total Pu	219 ± 38.4 μg/L
Np-237	567 ± 42.6 μg/L
total U	10 000 μg/L

adequate sampling of cation configurations, the problem of full sampling of cation degrees of freedom in a grand canonical ensemble simulation is a difficult one. Therefore, this simplified simulation was used as an initial check to determine whether cation motion would affect the amount of water adsorbed. The move probabilities for the simulations are given in Table 5. Subsequently, a canonical Replica Exchange Monte Carlo (REMC) simulation[31,32] was performed using the same relative translation and rotation probabilities. A total of 20 million steps were carried out, with the first 5 million discarded for equilibration. The replicas were spaced at temperature multiples of 1.1,[33] starting with a minimum temperature of 300 K and ending with a maximum temperature of 2686.3 K.

Radionuclide Sorption Studies. Testing of combined strontium and actinide removal performance was carried out at the Savannah River National Laboratory (SRNL) using a simulated waste solution having the composition as shown in Table 6 prepared using ACS research grade chemicals and ultrapure water (MilliQ Element) as previously described.[20] Uranyl nitrate hexahydrate (Mallinckrodt Lot #8640KDAL) and nitric acid solutions of neptunium(V) (67.1 g/L) and plutonium(IV) (19.3 g/L), which derive from neptunium and plutonium operations at the Savannah River Site. ^{85}Sr radiotracer (Perkin-Elmer Life Sciences Cat. #NEZ082) was added to the simulant to measure strontium removal by gamma counting. The oxidation state and speciation of neptunium and uranium in the simulant is $Np(V)O_2^+$ and Pu(IV), respectively.[34]

Strontium and actinide removal testing occurred at 25 + 3 °C at phase ratio of simulant (mL) to sorbent (g) of 1370 mL/g. Sampling of the test bottles occurred at 4, 24, and 168 h of contact. Samples were filtered through 0.45-μm syringe filters (nylon membrane) to remove sorbent solids. Gamma spectroscopy measured the ^{85}Sr and neptunium content in the filtered solutions. ^{85}Sr activities were decay corrected to the time of sampling. We measured the alpha activity, which is principally due to plutonium isotopes, by radiochemical separation of the plutonium from uranium and neptunium followed by alpha counting of the extracted plutonium. Sorption tests including a control test (no added sorbent) were run in parallel for comparison to the polyoxometalate sorption tests and confirm that loss of strontium and actinides did not occur by sorption onto container walls or filter surfaces.

Results and Discussion

The summary of exchange/sorption experiments performed on the different Keggin-chain phases are summarized in Table 7. The most complete set of experiments was carried out on **Ti-Si-Nb**, due to its greatest stability and ease of synthesis. We investigated strontium exchange because ^{90}Sr is a radionuclide of utmost concern in both tank wastes and as a contaminant in the environment, due to its high radioactivity and considerable mobility.[20,35–37] Ion exchange studies with Cd^{2+} and Yb^{3+} were executed in the interest of a representative transition metal and lanthanide, respectively. Many additional exchange experiments were also done with other metal salts, and according to qualitative compositional analysis (EDS), complete replacement of the metal of interest for sodium always occurs. This confirms the very mobile nature of the hydrated sodium cations that are interstitial to the Keggin chains. However, in many experiments, the ion exchange resulted in extensive diminishment of quality of the powder X-ray data, likely because of diminished periodic arrangement of the chains with irregular expansion or contraction of the interchain spacing. Therefore, no useful structural information was obtainable, and these experiments are not discussed further in this report; except to note the ease of ion-exchange in phases held together loosely only by the hydrated exchangeable cations in the (110) plane.

Sr-Exchange of Keggin Chain Materials. The unit cell parameters of the native sodium forms and the ion-exchanged forms of the four Keggin-chain phases are summarized in Table 1, where the unit cells of the native sodium forms have been reported prior.[15] The observed, calculated, and difference patterns of Sr-exchanged **Ti-Si-Nb** from Rietveld refinement is shown in Figure 2. For each of the compositions, there is an increase in the unit cell upon exchange of the sodium with strontium, by ~0.3 Å in both the *a*-direction and the *c*-direction, which gives around a 170–180 Å^3 increase in unit cell volume. We have identified three Sr sites, where Sr1 is fully occupied, accounting for 8 of the 12 Sr^{2+} necessary for charge-balancing in the unit cell (or per two Keggin clusters), and the 4 remaining Sr cations per unit cell are in partially occupied sites Sr2 and Sr3, where Sr2 is half-occupied and Sr3 is one-quarter occupied. The strontium sites are shown in the *c*-axis view in Figure 3. Sr1 is most highly coordinated to the Keggin-chain framework; it sits in a four-ring window of one Keggin ion, a bonding motif frequently observed in sodium and potassium salts of phases featuring the dodecaniobate Keggin ion.[15,17,38] Sr1 is further

(31) Hansmann, U. H. *Chem. Phys. Lett.* **1997**, *281*, 140–150.
(32) Beauvais, C.; Guerrault, X.; Coudert, F. X.; Boutin, A.; Fuchs, A. H. *J. Phys. Chem. B* **2004**, *108*, 399–404.
(33) Kofke, D. A. *J. Chem. Phys.* **2002**, *117*, 6911–6914.
(34) Duff, M. C.; Hunter, D. B.; Hobbs, D. T.; Barnes, M. J.; Fink, S. D. *Characterization of Sorbed Actinides on Monosodium Titanate*; WSRC-TR-2-1-00467; Westinghouse Savannah River Company: Aiken, SC, Oct 12001.
(35) Nyman, M.; Hobbs, D. T. *Chem. Mater.* **2006**, *18*, 6425–6435.
(36) Bowers, G. M.; Ravella, R.; Komarneni, S.; Mueller, K. T. *J. Phys. Chem. B* **2006**, *110*, 7159–7164.
(37) McKinley, J. P.; Zachara, J. M.; Smith, S. C.; Liu, C. *Geochim. Cosmochim. Acta* **2007**, *71*, 305–325.

Table 7. Summary of Ion-Exchange and Sorption Studies on Keggin-Chain Materials

	experiment				
phase	Sr-exchange-complete	Sr-exchange—substoichiometic	Cd-exchange	Yb-exchange	Sr/actinide sorption from SRS simulant
Ti-Si-Nb	yes	yes	yes	yes	yes
Ti-Ge-Nb	yes	no	no	no	yes
Nb-Si-Nb	yes	no	no	no	yes
Nb-Ge-Nb	yes	no	no	no	yes

bonded to two terminal Nb-O_t (t = terminal) oxygens of adjacent ions, and two water molecules that reside in the only nonmobile water site that was located from X-ray diffraction data. All Sr−O bonds are ≤3.1 Å. Sr2 is bonded to two terminal Nb−O_t oxygens of clusters on adjacent chains, with almost a 180° O_t−Sr2−O_t bond angle. Sr3 sits near the Ti_2O_2 bridge between the Keggin ions and has four bonds to a single chain; one to a O_b−Ti_2 oxygen, one to a O_b−(Nb_2Ti) and two to Nb−$O_t$oxygen atoms. Both Sr2 and Sr3 likely are coordinated by mobile water molecules that are not located by X-ray diffraction, but predicted by the computational studies or corroboration with thermogravimetry (see below). Similarly, the native sodium form, discussed in detail in a prior publication, has a fully occupied sodium site that sits in a four-ring window and bonds to two terminal oxygen sites on adjacent clusters of a neighboring chain.[15] A second sodium site is between two O_b−Nb_2 oxygens of adjacent chains, a third sodium site is bonded to a O_b−Ti_2 oxygen and a terminal Nb−O_t oxygen, and the fourth sodium site is bonded to a single terminal oxygen, Nb−O_t only.

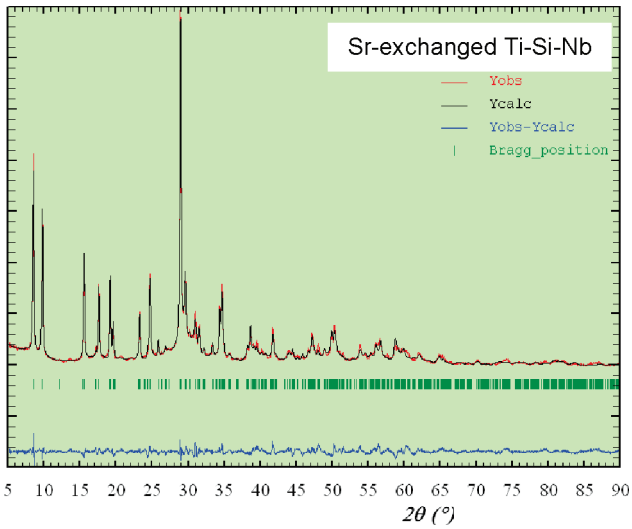

Figure 2. Observed, calculated, and difference spectra of Sr-exchanged **Ti-Si-Nb** from Rietveld structural refinement.

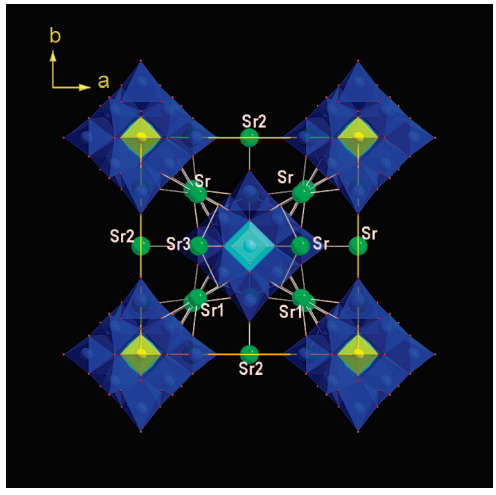

Figure 3. Representation of Sr-exchanged **Ti-Si-Nb** down the Keggin-chain axis (*c*-axis). Dark blue octahedra are NbO_6, yellow tetrahedra are SiO_4, light blue octahedra are TiO_6, and green spheres are strontium.

Like the native Na form of **Ti-Si-Nb**, only four water molecules per Keggin cluster were located in relatively immobile sites from the X-ray diffraction data. Also like the native Na form, thermogravimetry revealed more weight loss than would be observed if there were only four water molecules per Keggin cluster. Water molecules are the only reasonably expected volatile species, based on the synthesis method, as well as infrared spectroscopy of the Keggin chain materials. Figure 4 shows the TGA curves for the native Na form of **Ti-Si-Nb**, along with the Sr-exchanged **Ti-Si-Nb**. Four water molecules per cluster would give a total weight loss of around 2.9% for the Sr form, whereas we observe a weight loss of 12.2%, which corresponds with 19 water molecules per cluster. The native Na form has fewer water molecules per cluster (see Figure 3), around 14.5.[15] These mobile water molecules create undetectable change in the X-ray diffraction data in both the native Na form[15] as well as the ion-exchanged forms, and therefore cannot be found by Fourier synthesis.

On average, there are approximately 3.2 water molecules associated with each Sr^{2+} cation, and 1.2 water molecules associated with each Na^+ cation[15], which is consistent with the observation that Sr^{2+} with its higher energy of hydration than Na^+ is absorbed into ion exchange phases with a larger hydration sphere.[39] By thermogravimetric and X-ray analyses and charge-balancing requirements, there are a total of 50 extra-framework species per unit cell for the Sr-exchanged form and 53 extra-framework species per unit cell for the native Na form[15] of **Ti-Si-Nb**. Therefore the increase in unit

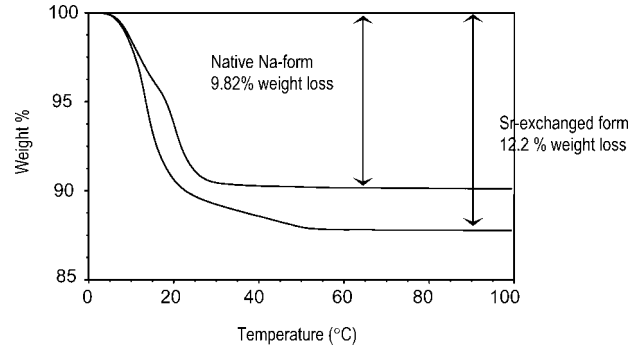

Figure 4. Thermogravimetric analysis (TGA) of the native Na form and the Sr-exchanged form of **Ti-Si-Nb**. The weight loss corresponds to 14.5 and 19 water molecules per cluster for the Na form and Sr-exchanged form, respectively.

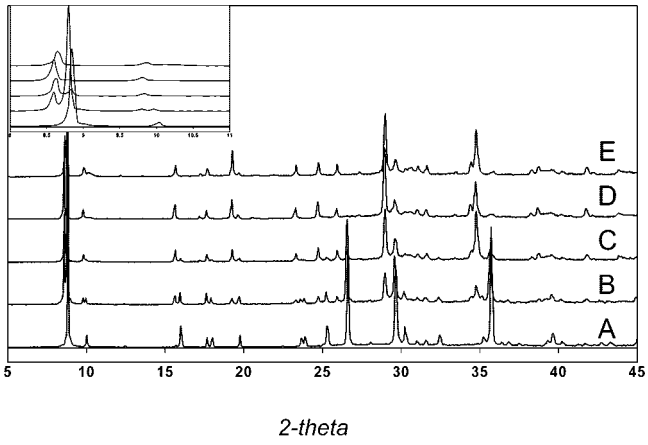

Figure 5. Powder X-ray diffraction spectra of **Ti-Si-Nb** (A) in its native sodium form, (B) 25% Sr exchanged, (C) 50% Sr exchanged, (D) 75% Sr exchanged, and (E) 100% Sr exchanged. Inset: expansion of low-angle region of spectrum.

cell for the Sr-exchanged form, 170 Å^3, cannot be accounted for by an increase in total extra-framework atoms. However, in the Sr-exchanged form, a larger percent of the extra-framework species are mobile (i.e more water molecules), which may account for the increase; i.e. mobile species require a larger volume than fixed species. The other factor to consider is the larger radius of the Sr^{2+} cation compared to the radius of the Na^+ cation.

A substoichiometric Sr exchange of **Ti-Si-Nb** gives a mixture of the native Na-form and the 100% Sr-exchanged form, rather than any intermediate exchange compositions; which was confirmed by Rietveld refinement of X-ray diffraction data of the intermediate exchange products. The X-ray diffraction patterns of the products of 0, 25, 50, 75 and 100% exchange shown in Figure 5 reveal two separate phases with unit cell parameters identical to those of the native Na and Sr-exchanged forms, rather than a single-phase with unit cell parameters intermediate between those of the Na- and Sr- end-members. These spectra were fitted with two-phase models of the Na and Sr end-members, with the ratios of the end-member phases proportional to the amount of Sr introduced into the exchange reaction.

Computational Results. The adsorption isotherm for water into the 100% Sr-exchanged **Ti-Si-Nb** at 300 K was computed with the Sr atoms fixed at their experimental positions. Figure 6 shows a plot of the amount of water adsorbed as a function of the ratio of water fugacity, f, to the saturation fugacity, f_{sat}. The maximum loading was found to be a little less than 16 water molecules per cluster, 15% fewer than was obtained experimentally. An additional simulation was conducted with the Sr atoms free to move, to verify that the water loading was not lowered significantly by simulation with fixed cations. This simulation yielded a slightly increased water loading of 16.1 water molecules per cluster. Sixteen water molecules would give a TGA result of 10.5% weight loss instead of the 12.2% observed. The error is likely to be experimental rather than computational.

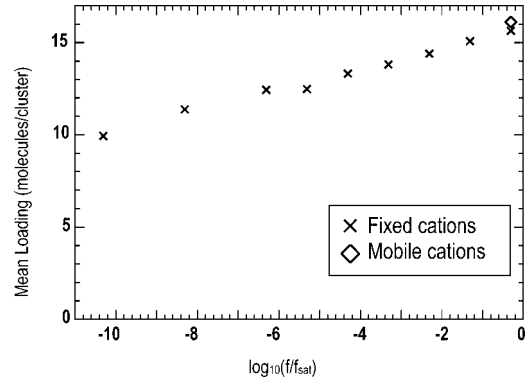

Figure 6. Computed amount of water adsorbed as a function of the ratio of simulated water fugacity to saturation fugacity for simple point charge water into 100% Sr-exchanged **Ti-Si-Nb**.

Table 8. Simulated Atomic Coordinates of Strontium Cations in 100% Sr-Exchanged Ti-Si-Nb Relative to Experimental Coordinates

site	Δx	Δy	Δz	standard dviation (Å)	deviation from experiment (Å)
Sr1	0.196	0.188	0.002	0.19	0.27
Sr2	−0.081	−0.034	0.150	0.90	0.17
Sr3	−0.002	−0.335	−1.40	0.50	1.44

The 1.7% difference could come from a small amount of decomposition of the Keggin chains (upon ion exchange) to hydrous niobium oxide (discussed later), or even some surface-adsorbed water.

Subsequent to the adsorption simulations, a canonical Replica Exchange (REMC) simulation was executed starting from the end configuration of the grand canonical simulation with mobile cations. The low-temperature replica at 300 K was analyzed to study cation and water locations and structure. The observed cation locations are reported in Table 8. The standard deviation is computed by measuring the fluctuations about the averaged position. The magnitude of this fluctuation gives an indication of the relative mobility of the Sr cation. The Sr1 and Sr2 sites showed excellent agreement with the experimental sites. However, the average Sr3 site was located 1.44 Å from the experimental position. Plots of Sr^{2+} coordinated to framework oxygen for fixed and mobile cations are shown in panels a and b in Figure 7, respectively. The coordination environment for site Sr1 is similar between the two simulations, with 5 oxygen atoms coordinated to Sr at a cutoff distance of 3 Å for both. Significant differences are observed for sites Sr2 and Sr3. When the cations are free to move, cations associated with site Sr3 coordinate more strongly with framework oxygen

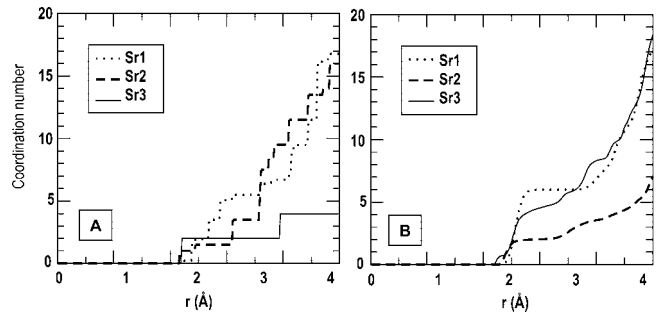

Figure 7. Sr^{2+} framework oxygen coordination, (a) fixed cations, (b) mobile cations from replica exchange Monte Carlo simulation.

(38) Nyman, M.; Bonhomme, F.; Alam, T. M.; Parise, J. B.; Vaughan, G. M. B. *Angew. Chem., Int. Ed.* **2004**, *43*, 2787–2792.
(39) Dontsova, K. M.; Norton, L. D.; Johnston, C. T.; Bigham, J. M. *Soil Sci. Soc. Am. J.* **2004**, *68*, 1218–1227.

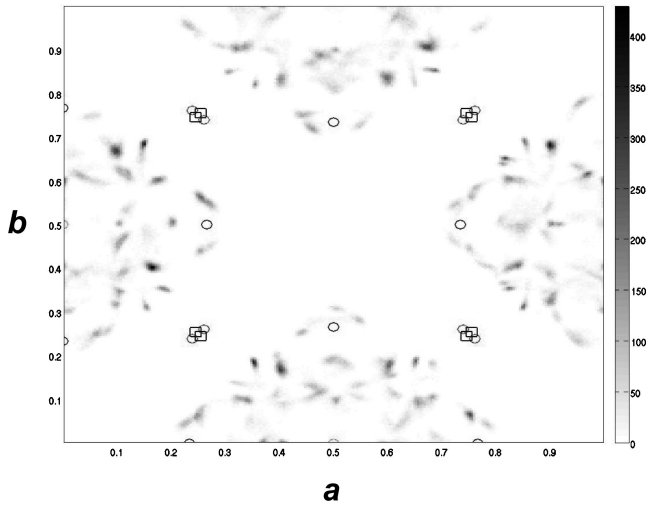

Figure 8. Projection of the distribution of water (from single point charge model) along the *c*-axis of 100% Sr-exchanged **Ti-Si-Nb** with fixed Sr^{2+} cations. Experimental cation positions are identified by circles, the proposed experimental water position Ow1 is identified by squares.

atoms, with an average of approximately four oxygen atoms within 3.1 Å. The greater degree of coordination in the mobile cation simulation is affected by a shift of the cations toward the oxygen atoms in the Ti−O−Ti bridge. In addition, a shift across the bridge is observed. In the region where this site is located, there are two pairs of terminal oxygen atoms, one pair on either side of the bridge. The experimental site Sr3 coordinates with one pair. In the simulation, however, the cations are observed to coordinate with the terminal oxygens on the cluster on the opposite side of the bridge. This discrepancy might be due to error in the location of the terminal oxygens, as the positioning of the cations is clearly sensitive to the oxygen positions. It may also be due to an error in the introduction of simulated disorder in the half-occupied bridging oxygen sites. We experienced a similar problem in inaccuracy of modeling K^+ ions near disordered framework oxygen sites in related linked Keggin-ion material, $K_{10}[Nb_2O_2][GeNb_{12}O_{40}]\cdot 11H_2O$.[17]

The low-temperature replica of the REMC simulation at 300 K and the GCMC simulation at saturation with fixed cations were also analyzed to study the regions where the water molecules were observed. A density map of the projection of water locations onto the a-b plane for fixed cations is shown in Figure 8. There were no notable differences observed with mobile cations. Although there is an observable degree of structure in the positioning of the water molecules, the population remains relatively diffuse. We can clearly see, however, that there was no water population at all observed at the location reported as the Ow1 site. In the experimental model, the Ow1 site alternates with Sr1 along the *c*-axis, at a bonding distance of 2.9 Å from Sr1. This behavior is consistent with previously simulations of related materials.[15]

Cd- and Yb-Exchange of Ti-Si-Nb. The unit cell parameters for Cd- and Yb exchanged **Ti-Si-Nb** are listed in Table 1, and the observed/calculated/difference spectra are shown in panels a and b in Figure 9. While Yb and Cd sites were assigned in the refinement (see the Supporting Information), we use these results primarily to document change in unit cell, because the diminishment of crystallinity of these phases decreases our confidence in the accuracy of assigned extra-framework positions. Cadmium exchange resulted in a decrease in the unit cell by around 125 $Å^3$, and ytterbium exchange resulted in almost the same unit cell as the native sodium form. The Cd-exchange experiment allowed characterization of exchanged-in cations by MAS NMR (magic angle spinning nuclear magnetic resonance) spectroscopy. The ^{113}Cd NMR spectrum of Cd-exchanged **Ti-Si-Nb** (Figure 10) has two peaks at −206 and −396 ppm in a 2:1 ratio. Like the Sr-exchanged phase, Cd-exchanged **Ti-Si-Nb** has a fully occupied Cd^{2+} site that coordinates in a 4-ring window of one cluster and bonds to two terminal oxygen-atoms of two additional clusters (Cd1, analogous to Sr1). The Cd−O bond lengths are shorter than Sr-O bond lengths (2.1–3.0 Å), thus the decrease in the unit-cell volume. We attribute the peak at −206 to the cation site that sits in the 4-ring window of the Keggin ion (eight per cluster). The peak at −396 ppm is assigned to the other two cation sites (total of four per cluster) that are less-coordinated to the framework and more highly coordinated to mobile water molecules.

Sr2+, U(IV), and $Np(V)O_2^+$ Separations into Keggin Chain Materials from Alkaline Nuclear Waste Stimulant. Figure 11 shows the concentration of Sr (7a), **Pu(IV)** (7b), and **$Np(V)O_2^+$** (7c) in the simulant as a function of contact time with the four Keggin chain materials, **Ti-Si-Nb**, **Ti-Ge-Nb**, **Nb-Si-Nb** and **Nb-Ge-Nb**. The Ti-bridged Keggin chain materials exhibited affinity for the sorption of Sr,

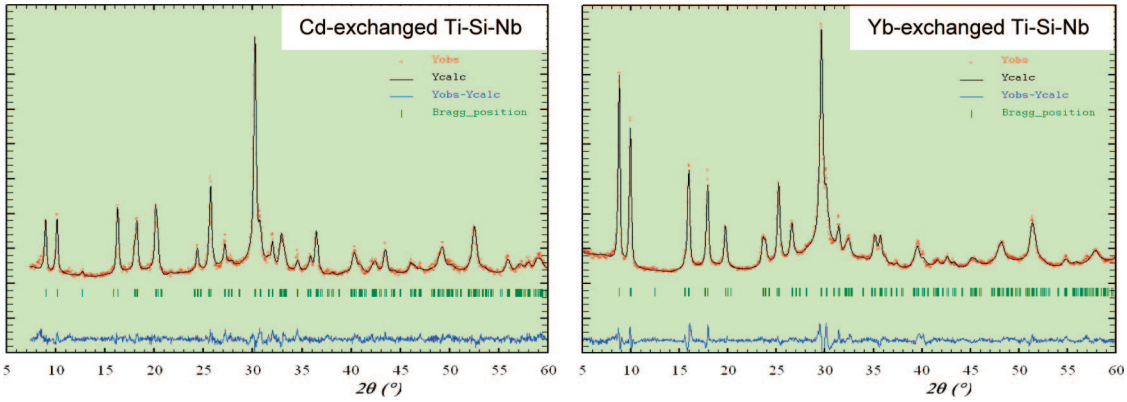

Figure 9. Observed, calculated, and difference X-ray diffraction spectra of Cd-exchanged (left) and Yb-exchanged (right) **Ti-Si-Nb**.

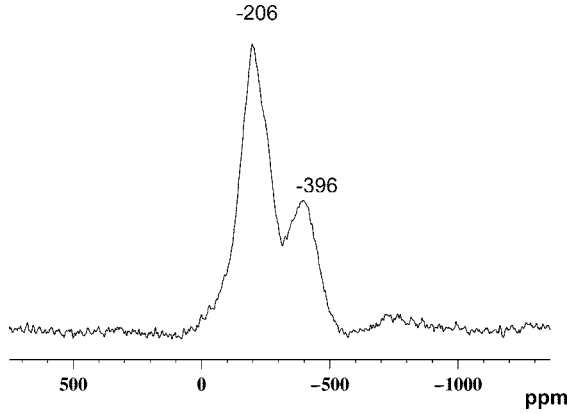

Figure 10. ^{113}Cd NMR spectrum of Cd-exchanged **Ti-Si-Nb**. The peaks at –206 and –396 ppm are present in a 2:1 ratio and attributed to the cation site that sits in the four-ring window of the Keggin ion (eight per cluster) and the other two cation sites (total of four per cluster), that are less coordinated to the framework and more highly coordinated to mobile water molecules.

Pu(IV), and $Np(V)O_2^+$. The Nb-bridged Keggin chain materials exhibited some affinity for Sr and $Np(V)O_2^+$ (albeit lower than that of the Ti-bridged materials) and no affinity for Pu(IV). For instance, the initial concentration of Sr in the simulant is 298 μg/L; after 168 h of contact (7 days) with the Keggin chain sorbent, the Sr concentration was reduced to 11 μg/L by **Ti-Si-Nb** and 48 μg/L by **Ti-Ge-Nb**. The two Nb-bridged Keggin chain materials reduced the Sr concentration to only around 168 μg/L in the same time period. The simulant featured an initial concentration of $Np(V)O_2^+$ concentration at 567 μg/L, which at 168 h contact time is reduced to 160 μg/L by **Ti-Ge-Nb** and 266 μg/L by **Ti-Si-Nb**. The Nb-bridged materials reduced the concentration to around 470 μg/L. Finally, the initial concentration of Pu(IV) in the simulant measured 219 μg/L, which reduced after 168 h of contact to 71.5 μg/L and 59.7 μg/L for the **Ti-Ge-Nb** and **Ti-Si-Nb** materials, respectively. The Nb-bridged Keggin chain materials exhibited no discernible sorption of Pu(IV).

We attribute the poorer performance of the Nb-bridged materials to the structural instability of the $[Nb_2O_2]^{6+}$ bridges, that has also been noted in the synthetic experiments of these materials.[15] A major decomposition product of the $[Nb_2O_2]^{6+}$ bridged Keggin chain materials is shorter chains or isolated clusters. We have observed this by characterization of precipitates from Keggin chain materials reacted with surfactants in aqueous media. Therefore conversion of the Keggin chains to isolated clusters or shorter chains may result in more rapid release of sorbed cations. However, isolated clusters or short chains of clusters may remove $Np(V)O_2^+$ from solution by a different mechanism; formation of insoluble Keggin- $Np(V)O_2^+$complexes in particular. Formation of insoluble complexes between tungstate Keggin ions and actinyl cations has certainly been observed.[40–43]

We have also observed that Ge-centered dodecaniobate Keggin ions are somewhat less stable the Si-centered

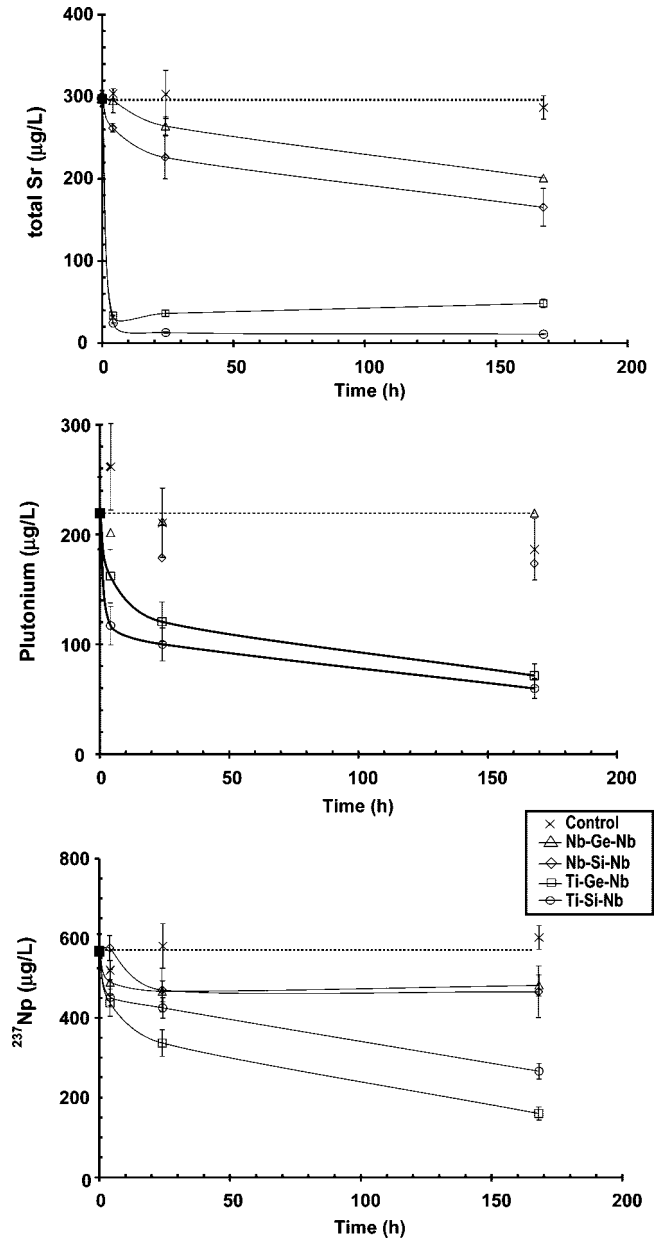

Figure 11. Concentration of total Sr, Pu, and ^{237}Np in Savannah River Site nuclear waste simulant with time upon contact with Keggin-chain phases. Data points are recorded at 4, 24, and 168 h (7 days). The dashed line is the control concentration of the radionuclide with no sorbent added.

analogues.[15,44] We expect the decomposition mechanism in this case involves actual decomposition of the Keggin ions to form amorphous Nb-oxide precipitates. The more stable **Ti-Si-Nb** composition exhibited greater affinity for Sr and Pu(IV), but surprisingly, poorer affinity for $Np(V)O_2^+$ compared to the less-stable **Ti-Ge-Nb** composition. This might be due to the different sorption behavior of the neptunyl species, $Np(V)O_2^+$, compared to Sr^{2+} and Pu(IV). While we know the Sr^{2+} exchanges with Na^+ into the intact Keggin chains as a hydrated cation and coordinates to the anionic framework; the chemical species, oxidation states,

(40) Saito, A.; Choppin, G. R. *Inorg. Chem.* **1991**, *30*, 4563.
(41) Saito, A.; Choppin, G. R. *J. Alloys Compd.* **1996**, *271/273*, 751.
(42) May, I.; Copping, R.; Cornet, S. M.; Talbot-Eeckelears, C. E.; Gaunt, A. J.; John, G. H.; Redmond, M. R.; Sharrad, C. A.; Sutton, A. D.; Collison, D.; Fox, O. D.; Jones, C. J.; Sarsfield, M. J.; Taylor, R. J. *J. Alloys Compd.* **2007**, *444*, 383.
(43) Choppin, G. R.; Wall, D. E. *J. Radioanal. Nucl. Chem.* **2003**, *255*, 47–52.
(44) Nyman, M.; Bonhomme, F.; Alam, T. M.; Parise, J. B.; Vaughan, G. M. B. *Angew. Chem., Int. Ed.* **2004**, *43*, 2787–2792.

complexation and exchange mechanism of the actinides are less well characterized and many more variations are possible compared to alkaline earth ions under strongly alkaline conditions.[45] In this study, perhaps amorphous niobium oxide is a better sorbent for $Np(V)O_2^+$ than it is for either Sr or Pu(IV).

Conclusions

Dodecaniobate Keggin-chain phases, $Na_{12}[Ti_2O_2][TNb_{12}O_{40}]\cdot xH_2O$ and $Na_{10}[Nb_2O_2][TNb_{12}O_{40}]\cdot xH_2O$ (T = Si, Ge), are intriguing ion-exchange materials. They have high exchange capacity (essentially 100% exchange of the Na^+ cations) and rapid exchange rates, since the both the lattice–water and cations are highly mobile in the interchain region. Selectivity (i.e., for Sr^{2+}) arises from the multidentate binding sites of the Keggin ions, such as the '4-ring windows' that readily bond cations through four framework oxygens. The coordinatively unsaturated terminal oxygen atoms of the Keggin ions are also involved in the coordination of extra-framework cations. However, the drawback of these phases lies in their structural instability, particularly the Nb-bridged phases. Complete characterization of the Sr-exchanged phases required molecular modeling, since the majority of the highly mobile water molecules do not reside on crystallographically defined sites. Molecular modeling was also helpful for confirming which extra-framework sites are most favorable for exchanged-in cations. Ion exchange of Yb^{3+} and Cd^{2+}, as well as a variety of other lanthanides and transition metals, demonstrated the great flexibility of these ion exchange phases. Selectivity for both Sr^{2+} and actinides was demonstrated in sorption tests using Savannah River Site Nuclear Waste simulant solutions.

In conclusion, the highly charged dodecaniobate Keggin ion (charge of −16) is ideal for self-assembling with cationic linkers into anionic frameworks. The Keggin ion geometry provides optimal binding sites for extra-framework cations; and furthermore, the one-dimensionally linked phases allows for high mobility of lattice water and ions. Finally, the base-stability of these materials means they can be utilized in applications such as treatment of highly caustic nuclear wastes. This combination of unique characteristics provides a foundation for an emerging family of ion exchange materials based on linked Keggin ions.

Acknowledgment. The authors thank the DOE EMSP (Environmental Management Science Program) for funding this work.

Supporting Information Available: CIF files for Sr-exchanged **Ti-Si-Nb**, **Nb-Si-Nb**, **Ti-Ge-Nb**, Cd-exchanged **Ti-Si-Nb**, and Yb-exchanged **Ti-Si-Nb**.

CM800158U

(45) Borkowski, M.; Lis, S.; Choppin, G. R. *Radiochim. Acta* **1996**, *74*, 117–121.